PNAS RESEARCH ARTICLE | NEUROSCIENCE

Deep brain stimulation in the subthalamic nucleus for Parkinson's disease can restore dynamics of striatal networks

Elie M. Adam[a,1], Emery N. Brown[a,b], Nancy Kopell[c,1,2], and Michelle M. McCarthy[c,1,2]

Contributed by Nancy Kopell; received November 17, 2021; accepted March 25, 2022; reviewed by Sabato Santaniello and Andrew Sharott

Deep brain stimulation (DBS) of the subthalamic nucleus (STN) is highly effective in alleviating movement disability in patients with Parkinson's disease (PD). However, its therapeutic mechanism of action is unknown. The healthy striatum exhibits rich dynamics resulting from an interaction of beta, gamma, and theta oscillations. These rhythms are essential to selection and execution of motor programs, and their loss or exaggeration due to dopamine (DA) depletion in PD is a major source of behavioral deficits. Restoring the natural rhythms may then be instrumental in the therapeutic action of DBS. We develop a biophysical networked model of a BG pathway to study how abnormal beta oscillations can emerge throughout the BG in PD and how DBS can restore normal beta, gamma, and theta striatal rhythms. Our model incorporates STN projections to the striatum, long known but understudied, found to preferentially target fast-spiking interneurons (FSI). We find that DBS in STN can normalize striatal medium spiny neuron activity by recruiting FSI dynamics and restoring the inhibitory potency of FSIs observed in normal conditions. We also find that DBS allows the reexpression of gamma and theta rhythms, thought to be dependent on high DA levels and thus lost in PD, through cortical noise control. Our study highlights that DBS effects can go beyond regularizing BG output dynamics to restoring normal internal BG dynamics and the ability to regulate them. It also suggests how gamma and theta oscillations can be leveraged to supplement DBS treatment and enhance its effectiveness.

basal ganglia | beta, gamma, and theta rhythms | medium spiny neurons | fast-spiking interneurons | correlated noise

Significance

Deep brain stimulation (DBS) in the subthalamic nucleus (STN) is highly effective for treating the motor symptoms of Parkinson's disease (PD). However, the neural mechanisms by which DBS acts are unknown. PD symptoms are tied to altered brain rhythms in basal ganglia (BG) and particularly the striatum. We develop a biophysical model of a BG neural pathway and show how beta oscillations can emerge throughout BG in PD. We then establish a mechanism by which DBS in STN can interrupt these abnormal rhythms and restore the brain's capability to produce and regulate normal rhythms lost with dopamine depletion. Our research suggests mechanisms to leverage striatal gamma and theta oscillations to counter aberrant dynamics and enhance the therapeutic effects of DBS.

Deep brain stimulation (DBS) in the subthalamic nucleus (STN), the sole excitatory nucleus of the basal ganglia, elicits a remarkable effect of rapidly restoring to almost normal, the very disabling motor symptoms of Parkinson's disease (PD). However, the mechanism of DBS efficacy remains a mystery. It is generally thought that DBS works though its systems-level effects on networks within and between the nuclei of the basal ganglia (BG), thalamus, and cortex (1). The motor symptoms of bradykinesia and rigidity are correlated with exaggerated beta frequency (~15 to 30 Hz) oscillations in STN local field potential (LFP) in PD patients (2, 3). Suppression of beta oscillations following high-frequency DBS to STN correlates with augmentation of motor function in PD patients (4). This suggests that some of the efficacy of high-frequency DBS in STN for PD symptoms may lie in the ability of DBS to reduce the pathologically elevated beta oscillations within the cortico-basal ganglia-thalamic (CBT) loop. Indeed, models have proposed a mechanistic role for DBS in STN in disrupting the propagation of aberrant oscillations to STN efferents (5) and normalizing output nuclei of the BG (6, 7). This normalization is found essential to restore relay reliability in the thalamus, which modeling suggests goes awry in Parkinsonian conditions due to abnormal BG output (8–11). Restoring thalamic reliability is likely an outcome of network interactions following DBS in STN, and it has been suggested that DBS engages a mechanism of converging network-wide input onto the striatum to achieve regularity of firing at the output of the BG (12). However, previous modeling work largely put the emphasis of the effects of DBS on the BG output and ignored its effect on internal BG dynamics. While restoring normal brain function indeed necessitates restoring reliable thalamocortical relay, matching the intricacies of action selection and voluntary motor control further requires the richness of the dynamics normally observed inside the BG nuclei.

Specifically, previous work from our group has shown that increased excitability in striatal medium spiny neurons (MSNs) expressing D2 receptors, which results from loss of dopamine (DA), increases beta oscillations in striatal networks (13) (see *Discussion* for the role of striatum in creating pathological beta). These beta oscillations are generated from inhibitory MSN interactions, in the presence of high cholinergic tone during PD. Thus, a DBS mechanism effective at restoring BG function, and more particularly striatal function, needs to be capable of rectifying this source of aberrant beta activity. No such mechanism has yet been studied nor proposed. Furthermore, beta (14–17),

Author affiliations: [a]Picower Institute for Learning and Memory, Massachusetts Institute of Technology, Cambridge, MA 02139; [b]Department of Anesthesia, Critical Care, and Pain Medicine, Massachusetts General Hospital, Boston, MA 02114; and [c]Department of Mathematics and Statistics, Boston University, Boston, MA 02215

Author contributions: E.MA., N.K., and M.M.M. designed research; E.M.A. performed research with input from E.N.B., N.K., and M.M.M.; and E.M.A., E.N.B., N.K., and M.M.M. wrote the paper.

Reviewers: S.S., University of Connecticut; and A.S., University of Oxford.

The authors declare no competing interest.

[1]To whom correspondence may be addressed. Email: eadam@mit.edu, nk@bu.edu, or mmccart@bu.edu.

[2]N.K. and M.M.M. contributed equally to this work.

This article contains supporting information online at https://www.pnas.org/lookup/suppl/doi:10.1073/pnas.2120808119/-/DCSupplemental.

Published May 2, 2022.

gamma ($\gtrsim$40 Hz) (18, 19), and theta ($\sim$4 to 8 Hz) oscillations (20, 21) are normally expressed in a DA-dependent manner in striatal networks to drive behavior, and the loss of DA in PD can disrupt the formation of these rhythms, as later shown. However, their coexistence may be necessary for normal behavioral function. The question we seek to answer is how striatal network level dynamics are restored, through DBS in STN, despite persisting cellular-level disruptions due to loss of DA. To answer this question, building on established computational models of striatum (13, 22), we explore network activity associated with a previously understudied but direct connection from STN to striatum (23–28). Recent research shows that the direct STN to striatum pathway projects strongly and almost exclusively to striatal fast-spiking interneurons (FSIs) (28).

There is uncertainty about the effect of DBS on STN and its efferents (29, 30). The major experimental evidence is that high-frequency stimulation (HFS) ($\gtrsim$100 Hz) of STN suppresses somatic activity through depolarization blockade (31, 32) and stimulates axonal terminals at a high frequency (33, 34). We modeled DBS in STN as a combination of these two aspects: DBS suppresses STN somatic activity, thereby suppressing the beta activity in STN, and replaces it with high-frequency activity at the level of STN axons. Our simulations show that HFS of the STN-FSI pathway fully restores striatal network dynamics including a reduction of beta and, most surprisingly, the reexpression of gamma and theta, striatal rhythms previously thought to be dependent on high levels of DA (22, 35–37). Moreover, our models suggest that the gamma/theta and beta dynamics can be modulated by cortical input during DBS, rather than by DA, thus allowing an alternative mechanism to DA modulation during task performance. The diverse functions of striatal networks are still elusive, but the network dynamics that underlie the possible functions have been widely reported and characterized (14–21). We thus confine our study of function restoration to an analysis of restoration of striatal dynamics and leave the complexity of how these dynamics enable various functions to further investigation. Our study further highlights how the parkinsonian STN can amplify beta in striatum and thus, throughout the CBT loop, via this direct feedback pathway to striatum. We find that DBS not only normalizes striatum but also interferes with this amplifying feedback loop by its dampening effect on STN somatic activity.

Results

BG Dynamics in Normal Conditions Show Intrinsically Generated Beta, Gamma, and Theta Oscillations. To study striatal dynamics, we developed a biophysical networked model of interacting neuronal populations in the BG and studied it in different conditions: normal, parkinsonian, and parkinsonian with DBS. DA levels fluctuate in normal conditions with effects on striatal dynamics. We refer to the baseline condition as the normal condition with baseline levels of DA and separately introduce a normal condition with high levels of DA.

The core of our model consisted of a striatal population of MSNs inhibited by FSIs. We further modeled a population of STN neurons projecting sparsely to the FSIs (Fig. 1*A*) and completed a loop in the BG by modeling a population of external globus pallidus (GPe) neurons that project to STN and receive MSN projections (Fig. 1*A*). This MSN-GPe-STN-FSI-MSN loop defines a neural pathway that partially goes through the indirect pathway of BG and offers the anatomical substrate for beta oscillations to be sustained and amplified, in PD. In baseline conditions, MSNs fire at an average rate (mean $\pm$ SD) of 1.21 ± 0.08 spk $\cdot$ s^{-1} (Fig. 1*B*). Overall, our model shows an absence of beta oscillations throughout the network, as evidenced by the spectra of the four populations (Fig. 1*C*). However, an isolated MSN network in baseline conditions does exhibit weak low-beta activity (13) (see *SI Appendix*, section A.1 and Fig. S1 *A–C* for details). But, in the core striatal model, we find that FSIs exhibit sparse gamma oscillations (22) (see *SI Appendix*, section A.2 and Fig. S1 *D–F* for details) that suppress MSN beta activity (see *SI Appendix*, section A.3 and Fig. S2 *A–C* for details). The behavior of the core striatal model remains unaltered when connected to the greater network comprising GPe and STN (see *SI Appendix*, section A.4 for details). The generation of beta in the MSNs is immediately suppressed by the FSIs and is not allowed to propagate throughout the loop.

Nevertheless, beta oscillations in normal condition do appear in MSNs, and the BG more generally, through bursts of beta activity (38–40), usually on the timescale of half of a single theta cycle ($\sim$150 ms) (39). At high DA levels, the FSI excitability and gap junction conductance are increased, pushing the FSIs to spike at nested theta/gamma oscillations (*SI Appendix*, Fig. S3*A*). FSI activity then comprises synchronized bursts of gamma activity, interleaved with quiescence, appearing at theta cycles, observed in spiking activity and in spectral content showing peaks at theta (7.27 ± 0.46 Hz) and gamma frequencies (77.23 ± 3.14 Hz). The bursts of gamma activity have the ability to momentarily suppress the MSN network, leaving it to rebound during the FSI quiescence period and generate bursts of beta oscillations (22). These theta-modulated bursts then appear in spiking activity and are also reflected in the aggregate population activity of MSNs. This activity mode emerges from the interactions in our core striatal model (*SI Appendix*, Fig. S3 *B–D*) and remains unaltered when connected to the greater network comprising GPe and STN. Synchronization of FSI activity into nested theta/gamma cycles is at the heart of enabling switches in cell assemblies representing different motor programs (18, 41), with beta oscillations sustaining cell assemblies (20, 42). We detail these results in later sections showing how DBS recovers such dynamics that are lost in PD.

Loss of Dopamine in PD Leads to Resonating Beta Activity throughout the BG. In PD, there are two effects that we included in our model: the loss of DA (43, 44) and the up-regulation of striatal cholinergic levels as a result of DA depletion (45–47). We modeled the changes in dopaminergic and cholinergic level through biophysical perturbations (Fig. 2*A*). We find that these changes result in an increase in beta frequency power in the striatum, the GPe, and the STN, consistent with what is observed clinically (13, 48–50).

Our simulations show that an isolated D2 MSN network (*SI Appendix*, Figs. S4 *A–C* and S5 *A–C*) and our core striatal model (*SI Appendix*, Fig. S5 *D–F*) produce beta oscillations during PD (see *SI Appendix*, section A.5 for details). Embedding our core striatal model into the closed loop (Fig. 2*A*), to include STN and GPe, amplifies beta-band activity during PD. We observe beta-band activity in all four populations MSN, FSI, STN, and GPe, directly through spiking activity (Fig. 2*B*) and through spectral power peaks in the beta band (at 15.80 ± 0.43 Hz in MSNs) (Fig. 2*C*) appearing in all four populations. The closed-loop system further creates resonance at beta frequencies as evidenced by additional power at harmonics, appearing in the spectra of population activity (Fig. 2*C*) (see *SI Appendix*, section A.6 for details). It is the increase of excitability of the MSNs that generates beta activity in the striatum (*SI Appendix*, Fig. S6 *A–D*) (see *SI Appendix*, section A.7 for details). This activity reaches the

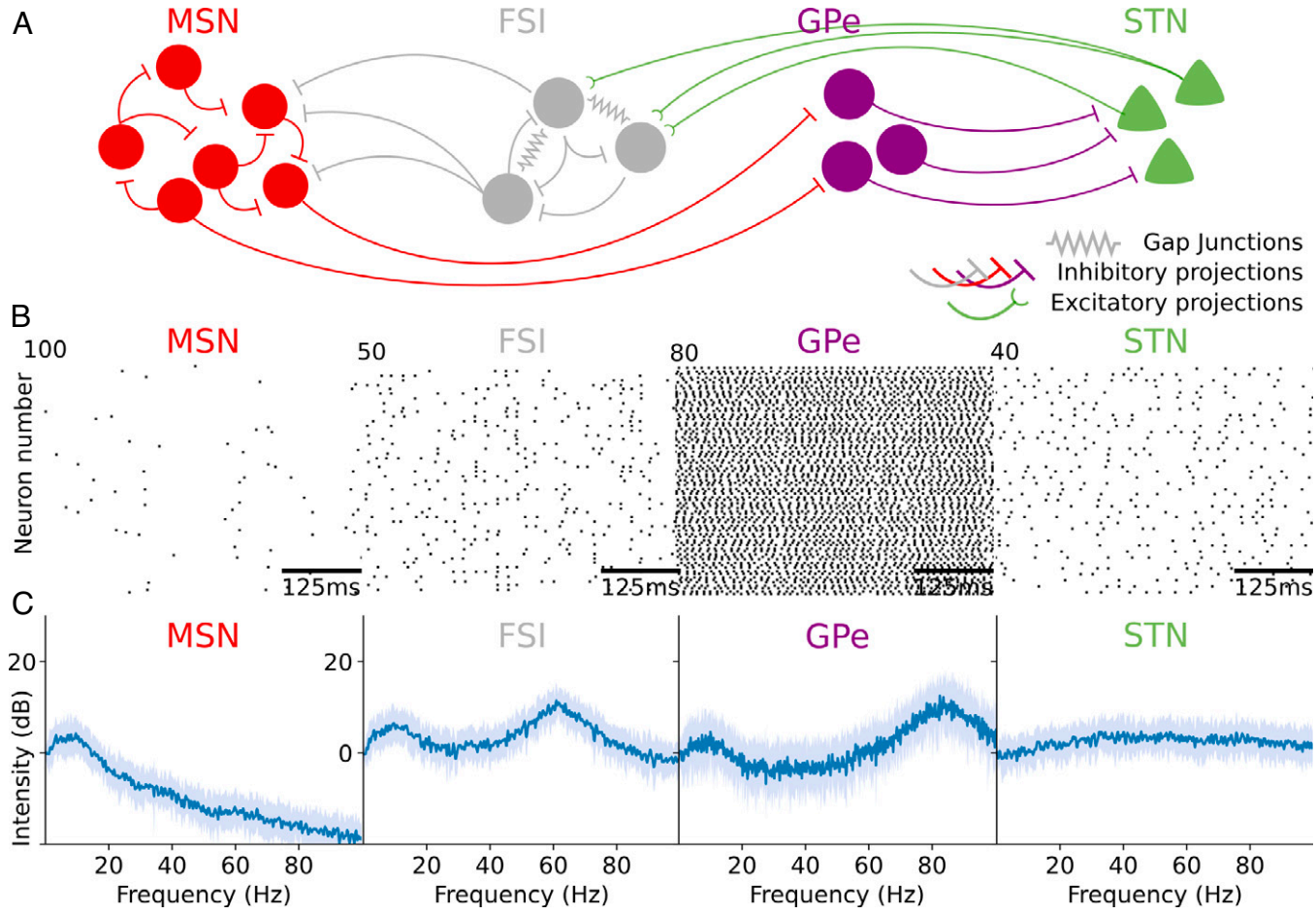

Fig. 1. Population dynamics in baseline condition. (*A*) Schematic illustrating the network structure of the biophysical neuronal model, composed of MSN, FSI, GPe, and STN neurons. (*B*) Raster plots showing spiking activity of MSN, FSI, GPe, and STN neurons, all in baseline condition (MSN firing rate: mean ± SD = 1.21 ± 0.08 spk $\cdot$ s^{-1}, $n = 25$ simulations). (*C*) Graphs showing the average (blue) and SD (light blue) of the spectra of the MSN, FSI, GPe, and STN population activity, all in baseline condition ($n = 25$ simulations).

weakened FSIs, through the STN and GPe (Fig. 2*B*), which in turns patterns the FSIs at beta frequencies (Fig. 2*C*). Instead of FSIs suppressing MSN beta activity via their sparse gamma, FSIs become a conduit for beta activity: The MSNs will resonate to the FSI beta inhibition due to their intrinsic and network dynamics, and beta activity is then amplified in MSNs and throughout the loop (see *SI Appendix*, section A.8 for details and *SI Appendix*, Figs. S7 *A–C* and S8 *A* and *B* for illustrations on resonance properties).

Our modeling suggests an intrinsic striatal origin of beta activity that is propagated throughout the BG loop in PD conditions, but we find a similar amplification of exogeneous beta under PD conditions. We investigated the effects of adding an exogenous beta activity directly into STN to model the two alternative sources. We find that an additional exogenous input into STN amplifies the existing beta oscillations throughout the loop if provided at the resonating frequency (*SI Appendix*, Fig. S9 *A* and *B*) and entrains the BG oscillations if not (*SI Appendix*, Fig. S9 *C–F*) (see *SI Appendix*, section A.9 for details). These results are consistent with experimental findings showing BG activity phase locking to cortical beta bursts in normal and parkinsonian conditions (40). Adding an exogenous beta input to MSNs instead of STN during PD also produces similar phenomena (*SI Appendix*, Fig. S10 *A–F*).

DBS in STN during PD Can Normalize MSN Activity by Restoring Effective FSI Inhibition. We modeled DBS in STN as a combination of two effects, considered in ref. 30: DBS suppresses somatic activity, thereby suppressing the beta activity derived from STN, and replaces it with high-frequency activity at the level of the axons (Fig. 3*A*). Essentially, DBS has the capability of decoupling STN axonal activity from STN somatic activity, thereby breaking beta oscillations in the BG loop and offering network excitation through HFS.

We modeled HFS by a train of voltage pulses subject to three parameters: 1) stimulation frequency, 2) stimulation voltage, and 3) pulse width. We fixed the applied voltage and varied the remaining two parameters: stimulation frequency and pulse width (see *SI Appendix*, section A.10 for details and an examination of an alternate model for DBS).

We find that DBS at 135 Hz with 150 μs pulse width during parkinsonian conditions normalizes MSN activity, lowering its firing rate to 1.31 ± 0.07 spk $\cdot$ s^{-1}, similar to what is observed in baseline conditions (Fig. 3*B*), and restoring its spectral properties to what is found in baseline conditions by removing the aberrant beta oscillations (Fig. 3*C*). We find that DBS achieves MSN activity normalization by altering FSI activity: The level of excitation in FSIs is increased, leading to higher spiking rates that include bursting at gamma frequencies (Fig. 3 *B* and *C*), and the gamma frequency of the FSI population follows around half of the stimulation frequency (at 67.1 ± 0.85 Hz for stimulation at 135 Hz) (corresponding to the peak in Fig. 3*C*).

We next find that FSIs can play a decisive role in determining the optimal frequency of DBS. As we vary the stimulation frequency, we find that the FSIs produce bursts at half of the stimulation frequency (Fig. 3*D*) (see *SI Appendix*, section A.11 and

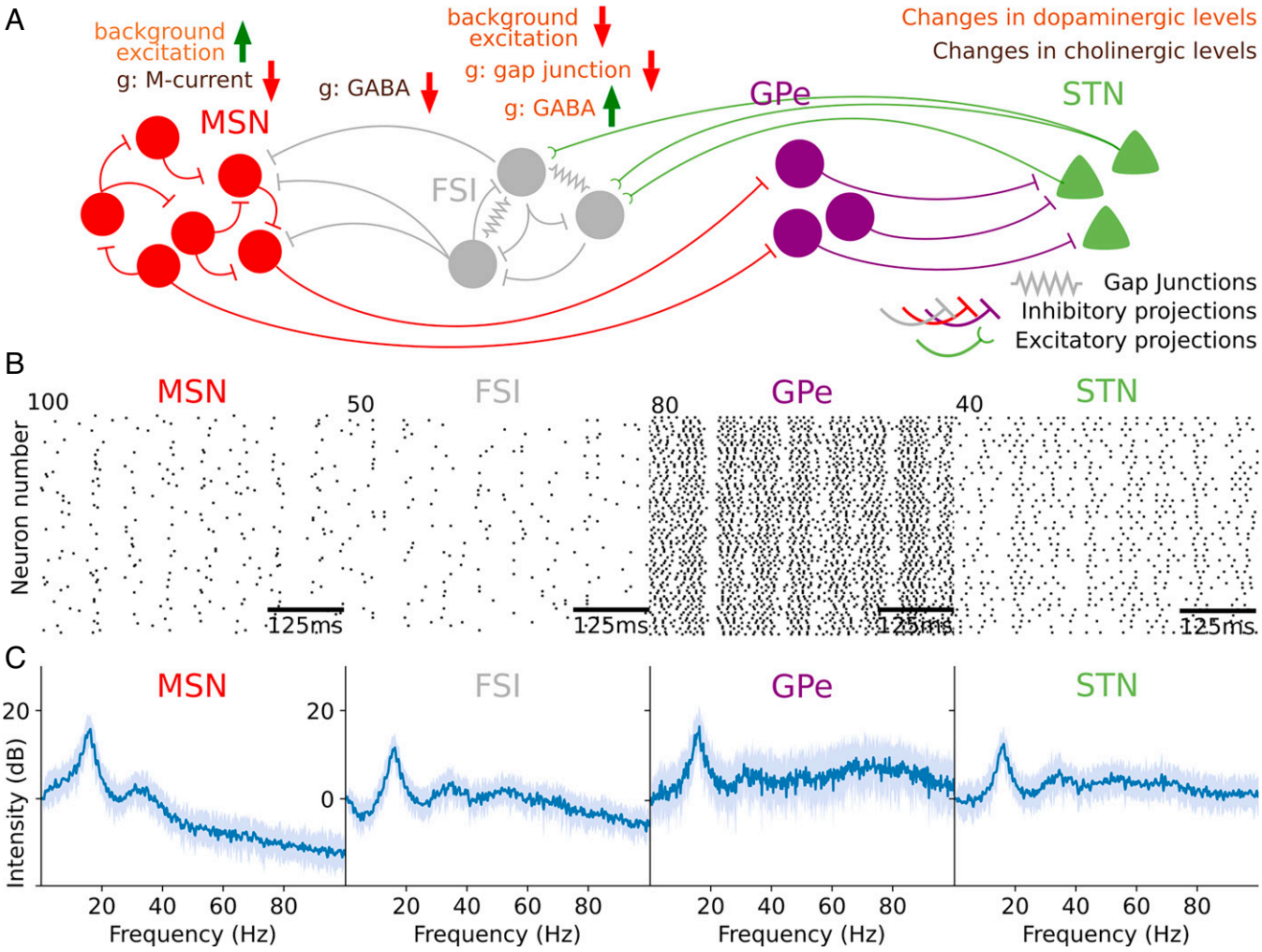

Fig. 2. Population dynamics in PD. (*A*) Schematic illustrating the parametric changes in the biophysical model in PD from parameters in baseline condition. The loss of DA is modeled in multiple ways: 1) an increase of background excitation onto the MSNs expressing D2 receptors (45), 2) a decrease in background excitation for FSIs (51), and 3) changes in effective connectivity among the FSIs [decreased electrical conductance for the gap junctions (52) and increase in their interneuronal GABAa maximal conductance (51)]. The increase in cholinergic tone 1) decreases the maximal MSN M-current conductance (via ACh action on M1 receptors) (45) and 2) decreases the inhibitory maximal conductance from FSIs to MSNs (53). (*B*) Raster plots showing spiking activity of MSN, FSI, GPe, and STN neurons, all in PD (MSN firing rate: mean ± SD = 4.85 ± 0.13 spk · s^{-1}, $n = 25$ simulations). (*C*) Graphs showing the average (blue) and SD (light blue) of the spectra of the MSN, FSI, GPe, and STN population activity, all in PD ($n = 25$ simulations).

Fig. S11*A* for details). Overall, increasing the DBS frequency also increases FSI firing rate (Fig. 3*E*) and thereby increases FSI-MSN inhibition, leading to a decrease in MSN firing rate (Fig. 3*F*) (see *SI Appendix*, section A.12 and Fig. S11 *B* and *C* for details). Thus, our model predicts that the optimal frequency for DBS will depend on the average MSN spiking rate in PD, a value that will vary by patient. Increasing the pulse width has a similar effect (see *SI Appendix*, section A.3 and Fig. S11 *D*–*F* for details).

In lower-frequency ranges, 60 Hz and upward, the FSIs oscillate at the DBS frequency (*SI Appendix*, Fig. S12 *A* and *B*: an example for DBS at 65 Hz), thereby justifying clinical improvement at these low frequencies too (54, 55) (*SI Appendix*, Fig. S12*A*, average MSN firing rate at 65 Hz: 1.65 ± 0.08 spk · s^{-1}). However, we show in a later section that such low frequencies fail to sustain theta/gamma FSI oscillations in PD conditions observed in normal dynamics under high levels of DA. Furthermore, stimulation at beta frequencies results in increased beta oscillation in MSNs (*SI Appendix*, Fig. S12 *C* and *D*) (average MSN firing rate at 5.57 ± 0.23 spk · s^{-1}, greater than that of MSNs in PD condition without DBS, $P < 0.001$, Welch's t test), which is consistent with findings showing worsening of symptoms (54, 56, 57).

DBS Restores Theta and Gamma Oscillations. At high DA levels in normal condition, FSI activity comprises synchronized bursts of gamma activity, interleaved with quiescence, appearing at theta cycles (22), clearly observed from the spiking activity (Fig. 4*A*) and the spectral content showing peaks at theta (7.27 ± 0.46 Hz) and gamma frequencies (77.23 ± 3.14 Hz) (Fig. 4*B*). The loss of DA during PD renders the FSIs unable to achieve such a dynamical state. This is partly due to a decreased excitation and an inability to synchronize in the presence of high beta noise with weakened gap junctions (see *SI Appendix*, section A.14 for details). However, we find that DBS increases FSI excitability and disrupts the beta noise coming into FSIs. This provides the opportunity for gamma bursts to arise, and that opportunity is governed by how well they are able to synchronize due to background noise. Indeed, background noise that is highly correlated among FSIs allows the FSIs to achieve synchrony, thereby replicating what is observed in conditions of high levels of DA, at the level of spiking activity (Fig. 4*C*) and spectral content (Fig. 4*D*) (gamma frequency at 66.81 ± 3.68 Hz and theta frequency at 6.11 ± 0.68 Hz). Background noise that is highly uncorrelated among FSIs would break synchrony and thus would replicate the conditions we observed in baseline normal condition (Fig. 1 *B* and *C*). This suggests that

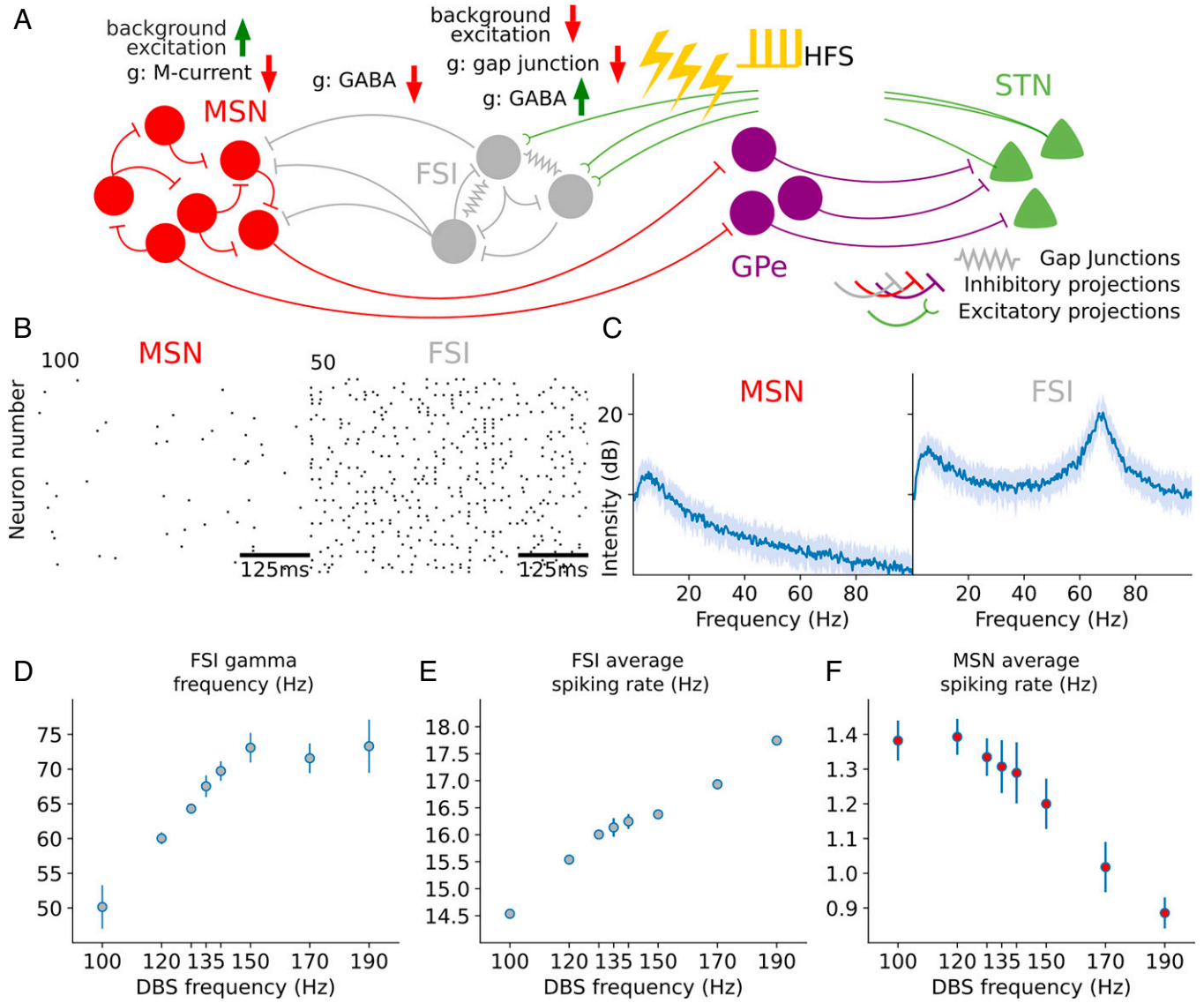

Fig. 3. Population dynamics during DBS in PD. (*A*) Schematic illustrating the parametric changes in the biophysical model in PD during DBS from parameters in baseline condition. (*B*) Raster plots showing spiking activity of MSN and FSI neurons, all in PD during DBS (MSN firing rate: mean ± SD = 1.31 ± 0.07 spk · s^{-1}, $n = 25$ simulations). (*C*) Graphs showing the average (blue) and SD (light blue) of the spectra of the MSN and FSI population activity, all in PD during DBS. (*D*) Graph showing the average FSI gamma oscillation frequency (bars representing SD) as a function of DBS frequency (10 simulations per simulated frequency). (*E*) Graph similar to *D* showing the average FSI firing rate as a function of DBS frequency. (*F*) Graph similar to *D* showing the average MSN firing rate as a function of DBS frequency.

DBS is able to substitute the mechanism of high/baseline DA, lost in PD, by a mechanism of correlated/uncorrelated noise to restore FSI and MSN dynamics.

We modeled the source of uncorrelated/correlated background noise to be coming from cortical input. We do not expect that mechanism of switching correlation to be one generated only in PD. Per our interpretation, in a regime of changing motor plans, we expect cortex to be engaged, with its activity correlated and conveyed to the striatum. This setting can coincide with high DA levels and deliver noise correlated among FSIs in normal conditions. In other regimes coinciding with baseline DA levels, cortical activity is uncorrelated and conveys only uncorrelated noise onto the FSIs. In normal conditions, however, the gap junctions are strong enough to overcome the noise whether it is uncorrelated or correlated. Therefore, although that functionality is always present, it need not be effectively used by the FSIs and can gain an effective use in PD during DBS, where DA levels are pathologically low. It also may be partially redundant in normal condition: Correlated noise promotes more synchrony among FSIs in normal condition, especially if the level of DA is low for some normal reason. However, the correlated noise by itself cannot bring the FSIs to robustly spike a theta/gamma without additional excitation onto the FSIs. This excitation is provided by a high level of DA in normal conditions and by DBS in PD, but can also be provided by phasic activity from thalamic/cortical projections.

Importantly, in PD conditions without DBS, it is not possible to recover synchronized theta/gamma oscillations in FSI population activity with correlated noise (Fig. 4 *E* and *F*), even if we input additional excitation (Fig. 4 *G* and *H*) (see *SI Appendix*, section A.15 for details).

DBS Restores Theta-Modulated Beta Bursts. At the level of MSNs during high DA conditions, the activity of D1 MSNs is increased, and D1 MSNs become a key player in the direct pathway of the BG. The activity of D2 MSNs is oppositely decreased. To study the effect of DBS on recreating MSN dynamics appearing in normal conditions with high DA, we then additionally modeled

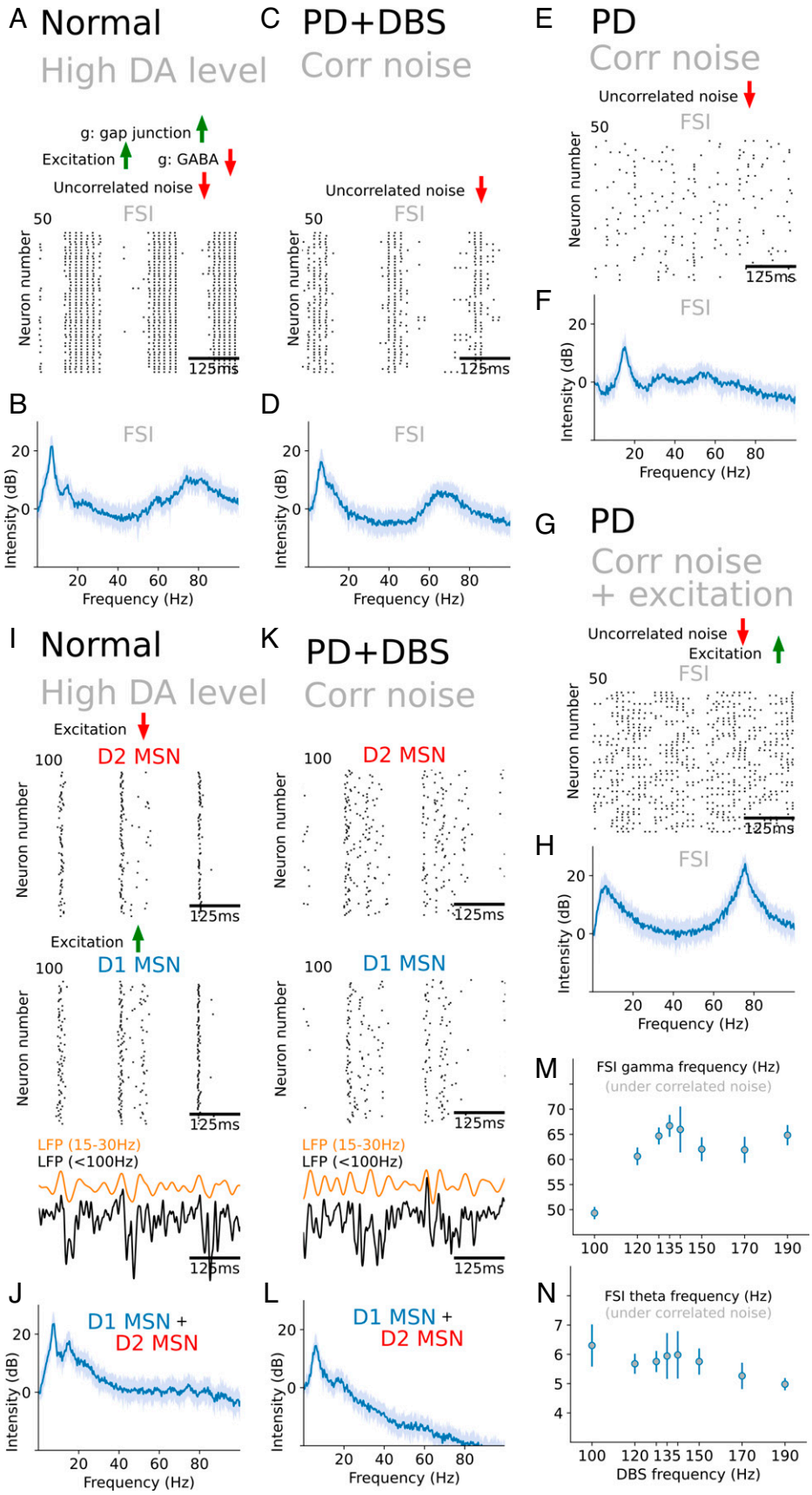

Fig. 4. DBS can restore the DA functionality lost during PD. (*A*) Raster plots showing spiking activity of FSI neurons, in normal conditions with high level of DA. (*B*) Graph showing the average (blue) and SD (light blue) of the spectrum of FSI population activity, in normal conditions with high level of DA. (*C* and *D*) Graphs displaying population activity of FSI neurons, as in *A* and *B*, but for PD with DBS and a synchronized noise regime. (*E*) Raster plots showing spiking activity of FSI neurons, in PD within a synchronized noise regime. (*F*) Graph showing the average (blue) and SD (light blue) of the spectrum of FSI population activity, in PD within a correlated noise regime. (*G* and *H*) Graphs displaying population activity of FSI neurons, as in *E* and *F*, but for PD within a correlated noise regime and added excitation for the FSIs to drive them individually at a theta/gamma oscillation. (*I* and *J*) Graphs displaying population activity of MSN neurons, as in *A* and *B*, for normal conditions with high level of dopamine. The raster plots show D1 and D2 MSN activity separately. Traces of raw (black) and beta-band filtered (orange) population activities of MSNs are additionally shown. (*K* and *L*) Graphs displaying population activity of MSN neurons, as in *I* and *J*, but for PD with DBS and a correlated noise regime. (*M*) Graph showing the average FSI gamma oscillation frequency (bars representing SD) as a function of DBS frequency under correlated noise conditions (10 simulations per simulated frequency). (*N*) Graph similar to *M* showing the average FSI theta oscillation frequency as a function of DBS frequency. All average spectra are derived from 25 simulations in each condition.

a population of D1 MSNs in our network. We modeled them to receive FSI projections, but they do not project to the GPe, as they are not considered canonically to be part of the indirect pathway of the BG. We also assumed that D1 and D2 MSNs are not interconnected by ionotropic γ-aminobutyric acid (GABAa) channels, to keep the role of D2 MSNs and their effect in our modeled indirect pathway loop unaltered.

In our simulations for normal conditions with high levels of DA, we found that both D1 and D2 MSNs were spiking when, and only when, FSIs were in their off cycle (Fig. 4*I*). These

bursts are produced at 7.21 ± 0.51 -Hz theta cycles (Fig. 4*I*) and exhibit beta oscillations (peak at 15.72 ± 0.72 Hz) in the short bursting period, as expected from disinhibited MSNs and observed through spiking activity (Fig. 4*I*) and spectral content of population activity (Fig. 4*J*). During PD with DBS under correlated noise, we found that this theta/beta firing of D1 and D2 MSNs is also preserved (theta frequency at 6.10 ± 0.62 Hz and beta frequency at 17.45 ± 1.09 Hz), as evidenced from the spiking activity (Fig. 4*J*) and spectral content (Fig. 4*L*). While beta activity is amplified in PD, it is not constant, but is modulated in amplitude in the form of frequent beta bursts with longer durations (40, 58, 59). By restoring FSI gamma bursts, DBS can shorten the MSN beta bursts to durations observed in normal conditions (on a theta timescale). Overall, in our model during PD, this modulation of beta activity to yield long bursts can be achieved by variations in MSN excitability, through exogenous cortical or thalamic input (e.g., *SI Appendix*, Fig. S13 *A–C* as an example). The phase locking of MSN beta activity to exogenous input directly to MSNs (*SI Appendix*, Fig. S10 *A–F*) or through STN (*SI Appendix*, Fig. S9 *A–F*) also suggests the potential for synchronization with cortical beta bursts as observed experimentally (40). In our simulations, D1 MSNs and D2 MSNs fire synchronously. Indeed, the D1 MSNs and D2 MSNs do not project to each other and receive FSI input with similar connectivity density. Adding mutual inhibition and asymmetric FSI projections will likely break the symmetry in MSN responses during the FSI off cycle, bringing them closer to experimental findings on pro- and antikinetic firing properties as well as coexistent firing activity in other conditions (60). We do not expect such a modification to alter the beta/theta activity pattern of the MSN populations, only the beta oscillation phase difference between the two MSN populations.

In the regime of synchronized noise, the DBS frequency also has an effect on the firing pattern of FSIs. We found that the FSI gamma firing also tracks the half frequency of the DBS stimulation frequency (Fig. 4*M*): The relation is linear within the range of 120 to 150 Hz, yet may break down outside this range. Furthermore, the theta frequency remains generally constant as DBS frequency changes (Fig. 4*N*). More importantly, while DBS at low frequencies (e.g., around 65 Hz) in uncorrelated noise conditions partially recovers dynamics observed in baseline condition (*SI Appendix*, Fig. S13 *C* and *D*), it is unable to recreate in FSIs theta/gamma dynamics in correlated noise conditions (*SI Appendix*, Fig. S14 *A* and *B*: example for DBS at 65 Hz) and thereby does not restore the theta-modulated beta bursts in MSNs (*SI Appendix*, Fig. S13 *C* and *D*). Indeed, stimulation at low frequencies does not raise the FSI excitation enough to yield bursts of gamma, as observed via FSI membrane potentials (*SI Appendix*, Fig. S13 *E–H*) or average firing rates (*SI Appendix*, Fig. S14*I*). FSI theta cycles are then not produced (*SI Appendix*, Fig. S14*J*). The effects of stimulation frequency on firing activity suggest that this parameter ought to be clinically adjusted to enable operation of natural FSI properties and ensure as close as possible natural dynamics, which will be patient specific. A thorough study of these effects is left for another investigation.

Discussion

Explaining the Mechanism of STN-DBS Action during PD. We show how DBS in STN can restore striatal dynamics in PD, by engaging an understudied subthalamo-striatal pathway to compensate and limit the effects due to DA depletion. The striatal populations naturally express beta, gamma, and theta oscillations (see *SI Appendix*, section C.1 and refs. 14–22, 36–39, 41, 42, and 61–84 for details). However, the loss of DA in PD leads to excessive beta oscillations in the striatum and an extinction of theta and gamma rhythms. We then find that DBS in STN can restore the natural dynamics in the striatum by engaging striatal interneurons to reverse the dynamical effects of DA depletion.

The effect of DBS is twofold: It interrupts the amplification of beta activity through the BG loop and provides FSIs with additional excitation through STN efferents. This relieves FSIs from having their activity contaminated by beta dynamics and allows them to express gamma oscillations via increased excitability, thereby restoring effective FSI to MSN inhibition. As such, DBS reverses D2 MSN overexcitability, which in turn leads to decreased beta oscillations throughout the BG. More essentially, we find that the functionality of DA in modulating dynamics—yielding theta and gamma oscillations and beta bursts—is restored, despite the absence of DA, through a different mechanism: dictated by the amount of correlation in cortico-striatal activity input.

Our work generally suggests the effects of DBS in normalizing dynamics and highlights a potentially crucial role for gamma oscillations in the behavioral recovery during PD.

Relation to Existing Insight on PD and DBS. While computational work on the mechanisms of DBS in STN has, thus far, focused on restoring normal functioning of BG output, notably the GPi (see *SI Appendix*, section C.2 and refs. 6–12 and 85–87 for details), our work focuses on restoring the dynamics of the BG nuclei, which then restores BG output dynamics. Our reasoning is that while output nuclei and thalamic functioning are essential to normal function, the intricacies of the mechanisms of action selection and switching motor programs, and their interaction with DA that is disrupted during PD, rely on the richness of BG rhythmic dynamics. Restoring striatal dynamics can then restore BG output function and thus reliability in thalamocortical relay.

Excessive beta oscillations extend throughout the CBT loop, and the source of beta generation in PD has been a contentious topic (see *SI Appendix*, section C.3 and refs. 48, 50, 70, 77, and 88–98 for details). Our view is that beta originates in the striatum (see *SI Appendix*, section C.4 and refs. 13, 88, 91, 96, 99, and 100 for details), possibly simultaneously combined with additional sources, e.g., from STN-GPe interaction (49, 101) and cortico-subthalamic patterning (49, 102, 103). The indirect pathway is particularly implicated in these beta dynamics (91), highlighting a special participation of MSNs in beta generation in rodents (88, 91) and in nonhuman primates (92). Yet, such findings are countered with reports that MSNs do not display beta oscillations in PD (95) and do not show increased firing (94) connected to beta, as also reported in the literature (93). It has also been argued that the striatum cannot produce the beta oscillation by itself because blockade of striatum to GPe does not eliminate the beta (97). Such contrasting conclusions suggest that the methodologies used as well as their interpretations need to be carefully evaluated (we discuss critiques of these points of view in *SI Appendix*, sections C.3 and C.4). Importantly, the interpretation of any such results will necessarily be dependent on an accurate representation of BG network pathways and cellular physiology. We elaborate on this point in *SI Appendix*, section B by studying alternate pathways—particularly via pallidostriatal and corticostriatal projections—through which STN activity can reach FSIs, examining their potential role during DBS and highlighting the special role played by the STN-FSI projection during DBS. Our current study highlights that even a minor pathway (the STN-to-FSI pathway) may prove to be a key component of system-level dynamics.

Our work further extends to address other beta sources, notably STN-GPe interaction and cortico-subthalamic patterning as previously mentioned: Beta propagation from these sources is automatically disrupted by STN somatic-axonal decoupling due to DBS. This further highlights the posited underlying mechanism of DBS effectiveness in disrupting abnormal information flow going through STN, formalized through the "disruption hypothesis" (104, 105). It is also pragmatic to expect DBS to operate on multiple fronts, each further alleviating PD symptoms. This is particularly the case as STN projects to a multitude of brain structures (see *SI Appendix*, section C.5 and refs. 34, 95, and 106–115 for details). We believe that similar mechanisms of modulation and normalization of dynamics, potentially engaging antidromic stimulation through HFS, can further arise at some of these identified fronts. Particularly, evidence for a key role for the GPe in regularizing dynamics is emerging (50, 70, 116–118).

Contributed Insight into PD and DBS. Our results illustrate how an STN locus for DBS can alter striatal dynamics and elucidate the efficacy of clinically considered stimulation frequencies as those resonating with striatal gamma dynamics. Furthermore, PD symptoms are presented in light of abnormal oscillatory beta dynamics replacing the normal interaction of rhythmic dynamics in the basal ganglia. DBS treatment might at first suggest restoring regularity in activity, but that does not immediately translate to flexibility in dynamics, to allow a range of motor command expression. Our work suggests that the effect of DBS extends from regularizing firing (as highlighted for example by refs. 6, 85, and 86) to restoring mechanisms of activity modulation (enabled through FSI inhibition onto MSNs) to restore flexibility in dynamics and activity patterns.

While DBS has often been studied in the context of regularizing firing activity in BG nuclei, compensating for one effect of DA loss, it has not been studied in light of how it can compensate for the dynamical modulatory effects of DA. Dopaminergic modulation is lost during PD, disrupting the ability of FSIs to synchronize and provide gamma bursts. However, our results show that DBS allows striatal FSIs to substitute the mechanism of dopaminergic control by that of cortical noise control. Once DBS reduces the beta activity that FSIs receive as input from the BG, cortical input becomes the major FSI provider of noise, and its correlation among FSIs dictates whether or not FSIs fire in synchrony. Crucially, in normal conditions, we consider high cortical activity correlation to coincide with high DA levels, thus yielding an adequate substitution in PD. This result is reminiscent of mathematical results on correlated noise-induced synchrony, where synchrony is achieved in coupled excitable systems (e.g., neurons coupled by gap junctions) at certain levels of correlated noise, but breaks at lower and higher intensity of noise (119–121). While correlated noise can aid in sustaining synchronous theta/gamma firings among FSIs during DBS in PD, it can additionally increase beta synchrony at the level of FSIs during PD in the absence of DBS (see *SI Appendix*, section C.6 and ref. 122 for details).

Potential Clinical Implications for Stimulus Design. Our work connects stimulation frequency, intensity, and pulse width to biophysical mechanisms potentially underlying the efficacy of DBS in STN. Our simulations yield optimal restoration of dynamics within the clinical ranges of these parameters (123). While increases in intensity and pulse width would increase the general level of excitation onto FSIs (see *SI Appendix*, section C.7 and refs. 54, and 123–128 for details), the effect of frequency appears to be much more intricate. The literature reports significant beneficial effects for stimulation frequencies ranging from 50 to 185 Hz, with the most beneficial effects reported within the 130- to 185-Hz range (54, 55). We find that increasing stimulation frequency increases FSI excitation, leading to increased FSI inhibition onto MSN, which may yield MSN firing rates lower than those of baseline dynamics. We also find that decreasing stimulation frequency interferes with gamma burst production in FSIs. We can then expect optimal DBS clinical effectiveness when the stimulation frequency matches the natural oscillatory dynamics of FSIs in the gamma range (18, 22, 129) and can resonate with FSI behavior. In the ranges above 120 Hz, the FSIs oscillate at half of the stimulation frequency with an oscillation of 67.5 Hz achieved for stimulation at 135 Hz.

It remains essential to verify such predictions, and we propose three directions: 1) By measuring FSI activity while altering DBS frequency (e.g., by using voltage markers and fiberphotometry), we expect FSI gamma oscillations to follow half the stimulation frequency during DBS. 2) By increasing activity correlation in cortical projections to FSIs (e.g., by using optogenetics or electrical stimulation), we expect FSIs to synchronize and yield gamma bursts during DBS. 3) By reducing FSI activity during DBS (e.g., by using chemogenetic approaches), we expect inhibition onto MSNs to be reduced and strong beta oscillations to reemerge during DBS. If these predictions hold true, then variations in the choice of DBS frequency between patients may partly be due to individualistic differences in oscillatory gamma frequencies, which our model links to properties of the FSI D current. DBS parameter optimization might then benefit from a learning phase whereby natural oscillatory gamma dynamics might be gathered under dopaminergic medication, using appropriate recording methods. There has also been success in using irregular stimulation patterns to alleviate PD symptoms (130), and it becomes a question of future research whether such patterns might affect FSI dynamics.

Our work suggests that the high stimulation frequency is resonant with FSI oscillatory dynamics, and leveraging it is at the heart of the therapeutic effect of DBS. It may be possible to engage resonance in other frequency bands, by introducing additional frequencies multiplexed in the stimulation pattern during DBS. In particular, while the cortical noise control mechanism provides a mechanistic fix in restoring theta/gamma FSI oscillations, relying only on cortical control might prove to problematic, as it might be unable to sustain the necessary activity for a long period of time to enable sequential tasks. This is particularly relevant in speech fluidity, in which we find verbal fluency to be impaired with DBS in STN (131, 132). Additional theta stimulation, along with HFS, might prove to be an effective therapy to maintain the low oscillatory state. Overall, our work highlights a potentially essential role played by gamma oscillations in overcoming beta oscillations in PD. The principle of recruiting resonance in additional populations might also unlock therapies and directions that at least might further improve DBS effectiveness.

Materials and Methods

All neurons are modeled using a single compartment with Hodgkin–Huxley-type dynamics. The voltage change in each cell is described by $c_m \frac{dv}{dt} = -\sum I_{membrane} - \sum I_{synaptic} + I_{app} + I_{noise}$.

All cells display a fast sodium current (I_{Na}), a fast potassium current (I_k), and a leak current (I_L) for membrane currents ($I_{membrane}$). MSNs additionally display an M current and FSIs additionally display a D current. The synaptic currents ($I_{synaptic}$) depend on the connectivity. The aggregate population activity of MSNs and of FSIs, from which spectral information was determined, consisted of the sum of GABAa synaptic currents between MSNs and between FSIs, respectively. The aggregate population activity of STN and GPe consisted of the sum of membrane potentials of STN and GPe cells, respectively. Modeling details are provided

in *SI Appendix*. Our network models were programmed in C++ and compiled using GNU gcc. The differential equations were integrated using a fourth-order Runge–Kutta algorithm. The integration time step was 0.05 ms. The model output was analyzed using Python 3.

Data Availability. All study data are included in this article and/or *SI Appendix*.

ACKNOWLEDGMENTS. This work was partially supported by NIH Award P01 GM118269 (to E.N.B. and N.K.).

1. C. C. McIntyre, P. J. Hahn, Network perspectives on the mechanisms of deep brain stimulation. *Neurobiol. Dis.* **38**, 329–337 (2010).
2. A. A. Kühn, A. Kupsch, G. H. Schneider, P. Brown, Reduction in subthalamic 8-35 Hz oscillatory activity correlates with clinical improvement in Parkinson's disease. *Eur. J. Neurosci.* **23**, 1956–1960 (2006).
3. A. A. Kühn *et al.*, Pathological synchronisation in the subthalamic nucleus of patients with Parkinson's disease relates to both bradykinesia and rigidity. *Exp. Neurol.* **215**, 380–387 (2009).
4. A. A. Kühn et al., High-frequency stimulation of the subthalamic nucleus suppresses oscillatory beta activity in patients with Parkinson's disease in parallel with improvement in motor performance. *J. Neurosci.* **28**, 6165–6173 (2008).
5. W. M. Grill, A. N. Snyder, S. Miocinovic, Deep brain stimulation creates an informational lesion of the stimulated nucleus. *Neuroreport* **15**, 1137–1140 (2004).
6. A. D. Dorval, A. M. Kuncel, M. J. Birdno, D. A. Turner, W. M. Grill, Deep brain stimulation alleviates parkinsonian bradykinesia by regularizing pallidal activity. *J. Neurophysiol.* **104**, 911–921 (2010).
7. K. Kumaravelu, D. T. Brocker, W. M. Grill, A biophysical model of the cortex-basal ganglia-thalamus network in the 6-OHDA lesioned rat model of Parkinson's disease. *J. Comput. Neurosci.* **40**, 207–229 (2016).
8. Y. Guo, J. E. Rubin, C. C. McIntyre, J. L. Vitek, D. Terman, Thalamocortical relay fidelity varies across subthalamic nucleus deep brain stimulation protocols in a data-driven computational model. *J. Neurophysiol.* **99**, 1477–1492 (2008).
9. Y. Guo, J. E. Rubin, Multi-site stimulation of subthalamic nucleus diminishes thalamocortical relay errors in a biophysical network model. *Neural Netw.* **24**, 602–616 (2011).
10. J. E. Rubin, D. Terman, High frequency stimulation of the subthalamic nucleus eliminates pathological thalamic rhythmicity in a computational model. *J. Comput. Neurosci.* **16**, 211–235 (2004).
11. R. Agarwal, S. V. Sarma, The effects of DBS patterns on basal ganglia activity and thalamic relay: A computational study. *J. Comput. Neurosci.* **33**, 151–167 (2012).
12. S. Santaniello *et al.*, Therapeutic mechanisms of high-frequency stimulation in Parkinson's disease and neural restoration via loop-based reinforcement. *Proc. Natl. Acad. Sci. U.S.A.* **112**, E586–E595 (2015).
13. M. M. McCarthy *et al.*, Striatal origin of the pathologic beta oscillations in Parkinson's disease. *Proc. Natl. Acad. Sci. U.S.A.* **108**, 11620–11625 (2011).
14. R. Courtemanche, N. Fujii, A. M. Graybiel, Synchronous, focally modulated beta-band oscillations characterize local field potential activity in the striatum of awake behaving monkeys. *J. Neurosci.* **23**, 11741–11752 (2003).
15. D. K. Leventhal *et al.*, Basal ganglia beta oscillations accompany cue utilization. *Neuron* **73**, 523–536 (2012).
16. H. N. Schwerdt *et al.*, Dopamine and beta-band oscillations differentially link to striatal value and motor control. *Sci. Adv.* **6**, eabb9226 (2020).
17. M. W. Howe, H. E. Atallah, A. McCool, D. J. Gibson, A. M. Graybiel, Habit learning is associated with major shifts in frequencies of oscillatory activity and synchronized spike firing in striatum. *Proc. Natl. Acad. Sci. U.S.A.* **108**, 16801–16806 (2011).
18. J. D. Berke, Functional properties of striatal fast-spiking interneurons. *Front. Syst. Neurosci.* **5**, 45 (2011).
19. M. A. van der Meer *et al.*, Integrating early results on ventral striatal gamma oscillations in the rat. *Front. Neurosci.* **4**, 300 (2010).
20. J. D. Berke, M. Okatan, J. Skurski, H. B. Eichenbaum, Oscillatory entrainment of striatal neurons in freely moving rats. *Neuron* **43**, 883–896 (2004).
21. L. Lalla, P. E. R. Orozco, M. T. Jurado-Parras, A. Brovelli, D. Robbe, Local or not local: Investigating the nature of striatal theta oscillations in behaving rats. *eNeuro* **4**, ENEURO.0128-17.2017 (2017).
22. J. A. K. Chartove, M. M. McCarthy, B. R. Pittman-Polletta, N. J. Kopell, A biophysical model of striatal microcircuits suggests gamma and beta oscillations interleaved at delta/theta frequencies mediate periodicity in motor control. *PLOS Comput. Biol.* **16**, e1007300 (2020).
23. R. M. Beckstead, A reciprocal axonal connection between the subthalamic nucleus and the neostriatum in the cat. *Brain Res.* **275**, 137–142 (1983).
24. H. Kita, S. T. Kitai, Efferent projections of the subthalamic nucleus in the rat: Light and electron microscopic analysis with the PHA-L method. *J. Comp. Neurol.* **260**, 435–452 (1987).
25. K. Nakano *et al.*, Topographical projections from the thalamus, subthalamic nucleus and pedunculopontine tegmental nucleus to the striatum in the Japanese monkey, Macaca fuscata. *Brain Res.* **537**, 54–68 (1990).
26. Y. Smith, L. N. Hazrati, A. Parent, Efferent projections of the subthalamic nucleus in the squirrel monkey as studied by the PHA-L anterograde tracing method. *J. Comp. Neurol.* **294**, 306–323 (1990).
27. Y. Koshimizu, F. Fujiyama, K. C. Nakamura, T. Furuta, T. Kaneko, Quantitative analysis of axon bouton distribution of subthalamic nucleus neurons in the rat by single neuron visualization with a viral vector. *J. Comp. Neurol.* **521**, 2125–2146 (2013).
28. K. Kondabolu *et al.*, A selective projection from the subthalamic nucleus to parvalbumin-expressing interneurons of the striatum. bioRxiv [Preprint] (2020). https://doi.org/10.1101/2020.11.26.400242 (Accessed 1 November 2021).
29. C. Hamani *et al.*, Subthalamic nucleus deep brain stimulation: Basic concepts and novel perspectives. *eNeuro* **4**, ENEURO.0140-17.2017 (2017).
30. C. C. McIntyre, W. M. Grill, D. L. Sherman, N. V. Thakor, Cellular effects of deep brain stimulation: Model-based analysis of activation and inhibition. *J. Neurophysiol.* **91**, 1457–1469 (2004).
31. A. Benazzouz *et al.*, Effect of high-frequency stimulation of the subthalamic nucleus on the neuronal activities of the substantia nigra pars reticulata and ventrolateral nucleus of the thalamus in the rat. *Neuroscience* **99**, 289–295 (2000).
32. C. Beurrier, B. Bioulac, J. Audin, C. Hammond, High-frequency stimulation produces a transient blockade of voltage-gated currents in subthalamic neurons. *J. Neurophysiol.* **85**, 1351–1356 (2001).
33. M. E. Anderson, N. Postupna, M. Ruffo, Effects of high-frequency stimulation in the internal globus pallidus on the activity of thalamic neurons in the awake monkey. *J. Neurophysiol.* **89**, 1150–1160 (2003).
34. T. Hashimoto, C. M. Elder, M. S. Okun, S. K. Patrick, J. L. Vitek, Stimulation of the subthalamic nucleus changes the firing pattern of pallidal neurons. *J. Neurosci.* **23**, 1916–1923 (2003).
35. J. D. Berke, Fast oscillations in cortical-striatal networks switch frequency following rewarding events and stimulant drugs. *Eur. J. Neurosci.* **30**, 848–859 (2009).
36. J. López-Azcárate *et al.*, Delta-mediated cross-frequency coupling organizes oscillatory activity across the rat cortico-basal ganglia network. *Front. Neural Circuits* **7**, 155 (2013).
37. N. Doñamayor, M. A. Schoenfeld, T. F. Münte, Magneto- and electroencephalographic manifestations of reward anticipation and delivery. *Neuroimage* **62**, 17–29 (2012).
38. R. Bartolo, H. Merchant, β oscillations are linked to the initiation of sensory-cued movement sequences and the internal guidance of regular tapping in the monkey. *J. Neurosci.* **35**, 4635–4640 (2015).
39. J. Feingold, D. J. Gibson, B. DePasquale, A. M. Graybiel, Bursts of beta oscillation differentiate postperformance activity in the striatum and motor cortex of monkeys performing movement tasks. *Proc. Natl. Acad. Sci. U.S.A.* **112**, 13687–13692 (2015).
40. H. Cagnan *et al.*, Temporal evolution of beta bursts in the parkinsonian cortical and basal ganglia network. *Proc. Natl. Acad. Sci. U.S.A.* **116**, 16095–16104 (2019).
41. M. Duhne *et al.*, Activation of parvalbumin-expressing neurons reconfigures neuronal ensembles in murine striatal microcircuits. *Eur. J. Neurosci.* **53**, 2149–2164 (2021).
42. A. K. Engel, P. Fries, Beta-band oscillations–signalling the status quo? *Curr. Opin. Neurobiol.* **20**, 156–165 (2010).
43. W. Poewe *et al.*, Parkinson disease. *Nat. Rev. Dis. Primers* **3**, 1–21 (2017).
44. T. Wichmann, Y. Smith, J. Vitek, "Pathophysiology of Parkinson's disease" in *Basal Ganglia Anatomy and Physiology*, S. A. Factor, W. J. Weiner, Eds. (Demos Medical Publishing, New York, 2002), pp. 245–265.
45. A. C. Kreitzer, Physiology and pharmacology of striatal neurons. *Annu. Rev. Neurosci.* **32**, 127–147 (2009).
46. P. DeBoer, M. J. Heeringa, E. D. Abercrombie, Spontaneous release of acetylcholine in striatum is preferentially regulated by inhibitory dopamine D2 receptors. *Eur. J. Pharmacol.* **317**, 257–262 (1996).
47. Y. Ikarashi, A. Takahashi, H. Ishimaru, T. Arai, Y. Maruyama, Regulation of dopamine D1 and D2 receptors on striatal acetylcholine release in rats. *Brain Res. Bull.* **43**, 107–115 (1997).
48. P. Brown, "Bad oscillations in Parkinson's disease" in *Parkinson's Disease and Related Disorders* (Springer, Vienna, 2006), vol. 70, pp. 27–30.
49. M. D. Bevan, P. J. Magill, D. Terman, J. P. Bolam, C. J. Wilson, Move to the rhythm: Oscillations in the subthalamic nucleus-external globus pallidus network. *Trends Neurosci.* **25**, 525–531 (2002).
50. N. Mallet *et al.*, Parkinsonian beta oscillations in the external globus pallidus and their relationship with subthalamic nucleus activity. *J. Neurosci.* **28**, 14245–14258 (2008).
51. E. Bracci, D. Centonze, G. Bernardi, P. Calabresi, Dopamine excites fast-spiking interneurons in the striatum. *J. Neurophysiol.* **87**, 2190–2194 (2002).
52. S. P. Onn, A. A. Grace, Dye coupling between rat striatal neurons recorded in vivo: Compartmental organization and modulation by dopamine. *J. Neurophysiol.* **71**, 1917–1934 (1994).
53. T. Koós, J. M. Tepper, Dual cholinergic control of fast-spiking interneurons in the neostriatum. *J. Neurosci.* **22**, 529–535 (2002).
54. M. Rizzone *et al.*, Deep brain stimulation of the subthalamic nucleus in Parkinson's disease: Effects of variation in stimulation parameters. *J. Neurol. Neurosurg. Psychiatry* **71**, 215–219 (2001).
55. E. Moro *et al.*, The impact on Parkinson's disease of electrical parameter settings in STN stimulation. *Neurology* **59**, 706–713 (2002).
56. A. Eusebio *et al.*, Effects of low-frequency stimulation of the subthalamic nucleus on movement in Parkinson's disease. *Exp. Neurol.* **209**, 125–130 (2008).
57. E. W. Tsang *et al.*, Subthalamic deep brain stimulation at individualized frequencies for Parkinson disease. *Neurology* **78**, 1930–1938 (2012).
58. G. Tinkhauser *et al.*, Beta burst dynamics in Parkinson's disease OFF and ON dopaminergic medication. *Brain* **140**, 2968–2981 (2017).
59. G. Tinkhauser *et al.*, Beta burst coupling across the motor circuit in Parkinson's disease. *Neurobiol. Dis.* **117**, 217–225 (2018).
60. S. Bariselli, W. C. Fobbs, M. C. Creed, A. V. Kravitz, A competitive model for striatal action selection. *Brain Res.* **1713**, 70–79 (2019).
61. D. Sochurkova, I. Rektor, Event-related desynchronization/synchronization in the putamen. An SEEG case study. *Exp. Brain Res.* **149**, 401–404 (2003).
62. B. C. Lega, M. J. Kahana, J. Jaggi, G. H. Baltuch, K. Zaghloul, Neuronal and oscillatory activity during reward processing in the human ventral striatum. *Neuroreport* **22**, 795–800 (2011).
63. E. G. Antzoulatos, E. K. Miller, Increases in functional connectivity between prefrontal cortex and striatum during category learning. *Neuron* **83**, 216–225 (2014).
64. K. Weineck, F. García-Rosales, J. C. Hechavarría, Neural oscillations in the fronto-striatal network predict vocal output in bats. *PLoS Biol.* **18**, e3000658 (2020).
65. J. Alegre-Cortés, M. Sáez, R. Montanari, R. Reig, Medium spiny neurons activity reveals the discrete segregation of mouse dorsal striatum. *eLife* **10**, e60580 (2021).
66. F. Kasanetz, L. A. Riquelme, M. G. Murer, Disruption of the two-state membrane potential of striatal neurones during cortical desynchronisation in anaesthetised rats. *J. Physiol.* **543**, 577–589 (2002).
67. M. A. Whittington, R. D. Traub, Interneuron diversity series: Inhibitory interneurons and network oscillations in vitro. *Trends Neurosci.* **26**, 676–682 (2003).
68. J. M. Schulz *et al.*, Enhanced high-frequency membrane potential fluctuations control spike output in striatal fast-spiking interneurones in vivo. *J. Physiol.* **589**, 4365–4381 (2011).
69. A. T. Popescu, D. Popa, D. Paré, Coherent gamma oscillations couple the amygdala and striatum during learning. *Nat. Neurosci.* **12**, 801–807 (2009).
70. T. O. West *et al.*, Propagation of beta/gamma rhythms in the cortico-basal ganglia circuits of the parkinsonian rat. *J. Neurophysiol.* **119**, 1608–1628 (2018).
71. B. Masimore, N. C. Schmitzer-Torbert, J. Kakalios, A. D. Redish, Transient striatal gamma local field potentials signal movement initiation in rats. *Neuroreport* **16**, 2021–2024 (2005).

72. N. Jenkinson, A. A. Kühn, P. Brown, γ oscillations in the human basal ganglia. *Exp. Neurol.* **245**, 72–76 (2013).
73. P. Brown, D. Williams, Basal ganglia local field potential activity: Character and functional significance in the human. *Clin. Neurophysiol.* **116**, 2510–2519 (2005).
74. M. P. Stenner *et al.*, Perimovement decrease of alpha/beta oscillations in the human nucleus accumbens. *J. Neurophysiol.* **116**, 1663–1672 (2016).
75. H. Tan, C. Wade, P. Brown, Post-movement beta activity in sensorimotor cortex indexes confidence in the estimations from internal models. *J. Neurosci.* **36**, 1516–1528 (2016).
76. Y. Zhang, X. Pan, R. Wang, M. Sakagami, Functional connectivity between prefrontal cortex and striatum estimated by phase locking value. *Cogn. Neurodyn.* **10**, 245–254 (2016).
77. R. M. Costa *et al.*, Rapid alterations in corticostriatal ensemble coordination during acute dopamine-dependent motor dysfunction. *Neuron* **52**, 359–369 (2006).
78. C. von Nicolai *et al.*, Corticostriatal coordination through coherent phase-amplitude coupling. *J. Neurosci.* **34**, 5938–5948 (2014).
79. W. E. DeCoteau *et al.*, Learning-related coordination of striatal and hippocampal theta rhythms during acquisition of a procedural maze task. *Proc. Natl. Acad. Sci. U.S.A.* **104**, 5644–5649 (2007).
80. J. E. Lisman, O. Jensen, The θ-γ neural code. *Neuron* **77**, 1002–1016 (2013).
81. W. E. DeCoteau *et al.*, Oscillations of local field potentials in the rat dorsal striatum during spontaneous and instructed behaviors. *J. Neurophysiol.* **97**, 3800–3805 (2007).
82. G. Buzsáki, Theta rhythm of navigation: Link between path integration and landmark navigation, episodic and semantic memory. *Hippocampus* **15**, 827–840 (2005).
83. M. E. Hasselmo, What is the function of hippocampal theta rhythm?–Linking behavioral data to phasic properties of field potential and unit recording data. *Hippocampus* **15**, 936–949 (2005).
84. A. B. Tort *et al.*, Dynamic cross-frequency couplings of local field potential oscillations in rat striatum and hippocampus during performance of a T-maze task. *Proc. Natl. Acad. Sci. U.S.A.* **105**, 20517–20522 (2008).
85. G. C. McConnell, R. Q. So, J. D. Hilliard, P. Lopomo, W. M. Grill, Effective deep brain stimulation suppresses low-frequency network oscillations in the basal ganglia by regularizing neural firing patterns. *J. Neurosci.* **32**, 15657–15668 (2012).
86. G. C. McConnell, R. Q. So, W. M. Grill, Failure to suppress low-frequency neuronal oscillatory activity underlies the reduced effectiveness of random patterns of deep brain stimulation. *J. Neurophysiol.* **115**, 2791–2802 (2016).
87. M. D. Humphries, K. Gurney, Network effects of subthalamic deep brain stimulation drive a unique mixture of responses in basal ganglia output. *Eur. J. Neurosci.* **36**, 2240–2251 (2012).
88. A. Singh, S. M. Papa, Striatal oscillations in Parkinsonian non-human primates. *Neuroscience*, **449**, 116–122.
89. M. Deffains *et al.*, Subthalamic, not striatal, activity correlates with basal ganglia downstream activity in normal and parkinsonian monkeys. *eLife* **5**, e16443 (2016).
90. D. D. Wang *et al.*, Subthalamic local field potentials in Parkinson's disease and isolated dystonia: An evaluation of potential biomarkers. *Neurobiol. Dis.* **89**, 213–222 (2016).
91. A. Sharott, F. Vinciati, K. C. Nakamura, P. J. Magill, A population of indirect pathway striatal projection neurons is selectively entrained to parkinsonian beta oscillations. *J. Neurosci.* **37**, 9977–9998 (2017).
92. L. Liang, M. R. DeLong, S. M. Papa, Inversion of dopamine responses in striatal medium spiny neurons and involuntary movements. *J. Neurosci.* **28**, 7537–7547 (2008).
93. A. Singh *et al.*, Human striatal recordings reveal abnormal discharge of projection neurons in Parkinson's disease. *Proc. Natl. Acad. Sci. U.S.A.* **113**, 9629–9634 (2016).
94. D. Valsky *et al.*, What is the true discharge rate and pattern of the striatal projection neurons in Parkinson's disease and dystonia? *eLife* **9**, e57445 (2020).
95. M. Deffains, L. Iskhakova, H. Bergman, Stop and think about basal ganglia functional organization: The pallido-striatal "stop" route. *Neuron* **89**, 237–239 (2016).
96. A. Singh, L. Liang, Y. Kaneoke, X. Cao, S. M. Papa, Dopamine regulates distinctively the activity patterns of striatal output neurons in advanced parkinsonian primates. *J. Neurophysiol.* **113**, 1533–1544 (2015).
97. Y. Tachibana, H. Iwamuro, H. Kita, M. Takada, A. Nambu, Subthalamo-pallidal interactions underlying parkinsonian neuronal oscillations in the primate basal ganglia. *Eur. J. Neurosci.* **34**, 1470–1484 (2011).
98. B. de la Crompe *et al.*, Publisher correction: The globus pallidus orchestrates abnormal network dynamics in a model of Parkinsonism. *Nat. Commun.* **11**, 1–14 (2020).
99. K. Kondabolu *et al.*, Striatal cholinergic interneurons generate beta and gamma oscillations in the corticostriatal circuit and produce motor deficits. *Proc. Natl. Acad. Sci. U.S.A.* **113**, E3159–E3168 (2016).
100. R. J. Moran *et al.*, Alterations in brain connectivity underlying beta oscillations in Parkinsonism. *PLOS Comput. Biol.* **7**, e1002124 (2011).
101. D. Plenz, S. T. Kital, A basal ganglia pacemaker formed by the subthalamic nucleus and external globus pallidus. *Nature* **400**, 677–682 (1999).
102. P. J. Magill, J. P. Bolam, M. D. Bevan, Dopamine regulates the impact of the cerebral cortex on the subthalamic nucleus-globus pallidus network. *Neuroscience* **106**, 313–330 (2001).
103. N. Yamawaki, I. M. Stanford, S. D. Hall, G. L. Woodhall, Pharmacologically induced and stimulus evoked rhythmic neuronal oscillatory activity in the primary motor cortex in vitro. *Neuroscience* **151**, 386–395 (2008).
104. S. Chiken, A. Nambu, High-frequency pallidal stimulation disrupts information flow through the pallidum by GABAergic inhibition. *J. Neurosci.* **33**, 2268–2280 (2013).
105. S. Chiken, A. Nambu, Mechanism of deep brain stimulation: Inhibition, excitation, or disruption? *Neuroscientist* **22**, 313–322 (2016).
106. C. Hamani, J. A. Saint-Cyr, J. Fraser, M. Kaplitt, A. M. Lozano, The subthalamic nucleus in the context of movement disorders. *Brain* **127**, 4–20 (2004).
107. J. L. Vitek, T. Hashimoto, J. Peoples, M. R. DeLong, R. A. Bakay, Acute stimulation in the external segment of the globus pallidus improves parkinsonian motor signs. *Mov. Disord.* **19**, 907–915 (2004).
108. M. Krause *et al.*, Deep brain stimulation for the treatment of Parkinson's disease: Subthalamic nucleus versus globus pallidus internus. *J. Neurol. Neurosurg. Psychiatry* **70**, 464–470 (2001).
109. R. Kumar *et al.*, Deep brain stimulation of the globus pallidus pars interna in advanced Parkinson's disease. *Neurology* **55** (suppl. 6), S34–S39 (2000).
110. A. Stefani *et al.*, Bilateral deep brain stimulation of the pedunculopontine and subthalamic nuclei in severe Parkinson's disease. *Brain* **130**, 1596–1607 (2007).
111. A. Saunders, K. W. Huang, B. L. Sabatini, Globus pallidus externus neurons expressing parvalbumin interconnect the subthalamic nucleus and striatal interneurons. *PLoS One* **11**, e0149798 (2016).
112. V. L. Corbit *et al.*, Pallidostriatal projections promote βoscillations in a dopamine-depleted biophysical network model. *J. Neurosci.* **36**, 5556–5571 (2016).
113. W. M. Grill, M. B. Cantrell, M. S. Robertson, Antidromic propagation of action potentials in branched axons: Implications for the mechanisms of action of deep brain stimulation. *J. Comput. Neurosci.* **24**, 81–93 (2008).
114. P. Ashby *et al.*, Potentials recorded at the scalp by stimulation near the human subthalamic nucleus. *Clin. Neurophysiol.* **112**, 431–437 (2001).
115. K. B. Baker, E. B. Montgomery Jr., A. R. Rezai, R. Burgess, H. O. Lüders, Subthalamic nucleus deep brain stimulus evoked potentials: Physiological and therapeutic implications. *Mov. Disord.* **17**, 969–983 (2002).
116. A. Abdi *et al.*, Prototypic and arkypallidal neurons in the dopamine-intact external globus pallidus. *J. Neurosci.* **35**, 6667–6688 (2015).
117. K. J. Mastro *et al.*, Cell-specific pallidal intervention induces long-lasting motor recovery in dopamine-depleted mice. *Nat. Neurosci.* **20**, 815–823 (2017).
118. T. A. Spix *et al.*, Population-specific neuromodulation prolongs therapeutic benefits of deep brain stimulation. *Science* **374**, 201–206 (2021).
119. J. D. Touboul, C. Piette, L. Venance, G. B. Ermentrout, Noise-induced synchronization and antiresonance in interacting excitable systems: Applications to deep brain stimulation in Parkinson's disease. *Phys. Rev. X* **10**, 011073 (2020).
120. P. Zhou, S. D. Burton, N. N. Urban, G. B. Ermentrout, Impact of neuronal heterogeneity on correlated colored noise-induced synchronization. *Front. Comput. Neurosci.* **7**, 113 (2013).
121. G. B. Ermentrout, R. F. Galán, N. N. Urban, Reliability, synchrony and noise. *Trends Neurosci.* **31**, 428–434 (2008).
122. S. Damodaran, J. R. Cressman, Z. Jedrzejewski-Szmek, K. T. Blackwell, Desynchronization of fast-spiking interneurons reduces β-band oscillations and imbalance in firing in the dopamine-depleted striatum. *J. Neurosci.* **35**, 1149–1159 (2015).
123. V. Dayal, P. Limousin, T. Foltynie, Subthalamic nucleus deep brain stimulation in Parkinson's disease: The effect of varying stimulation parameters. *J. Park. Disease* **7**, 235–245 (2017).
124. P. Sauleau *et al.*, Motor and non motor effects during intraoperative subthalamic stimulation for Parkinson's disease. *J. Neurol.* **252**, 457–464 (2005).
125. A. L. Törnqvist, L. Schalén, S. Rehncrona, Effects of different electrical parameter settings on the intelligibility of speech in patients with Parkinson's disease treated with subthalamic deep brain stimulation. *Mov. Disord.* **20**, 416–423 (2005).
126. E. Tripoliti *et al.*, Effects of subthalamic stimulation on speech of consecutive patients with Parkinson disease. *Neurology* **76**, 80–86 (2011).
127. G. Tommasi *et al.*, Pyramidal tract side effects induced by deep brain stimulation of the subthalamic nucleus. *J. Neurol. Neurosurg. Psychiatry* **79**, 813–819 (2008).
128. V. Dayal *et al.*, The effect of short pulse width settings on the therapeutic window in subthalamic nucleus deep brain stimulation for Parkinson's disease. *J. Park. Disease* **8**, 273–279 (2018).
129. D. Golomb *et al.*, Mechanisms of firing patterns in fast-spiking cortical interneurons. *PLOS Comput. Biol.* **3**, e156 (2007).
130. D. T. Brocker *et al.*, Optimized temporal pattern of brain stimulation designed by computational evolution. *Sci. Transl. Med.* **9**, eaah3532 (2017).
131. R. Cilia *et al.*, Brain networks underlining verbal fluency decline during STN-DBS in Parkinson's disease: An ECD-SPECT study. *Parkinsonism Relat. Disord.* **13**, 290–294 (2007).
132. A. Højlund, M. V. Petersen, K. S. Sridharan, K. Østergaard, Worsening of verbal fluency after deep brain stimulation in Parkinson's disease: A focused review. *Comput. Struct. Biotechnol. J.* **15**, 68–74 (2016).